



Superdense Coding over Optical Fiber Links with Complete Bell-State Measurements

Brian P. Williams,^{*} Ronald J. Sadlier,[†] and Travis S. Humble[‡]

Quantum Computing Institute, Oak Ridge National Laboratory, Oak Ridge, Tennessee 37831, USA

(Received 2 September 2016; published 1 February 2017)

Adopting quantum communication to modern networking requires transmitting quantum information through a fiber-based infrastructure. We report the first demonstration of superdense coding over optical fiber links, taking advantage of a complete Bell-state measurement enabled by time-polarization hyperentanglement, linear optics, and common single-photon detectors. We demonstrate the highest single-qubit channel capacity to date utilizing linear optics, 1.665 ± 0.018 , and we provide a full experimental implementation of a hybrid, quantum-classical communication protocol for image transfer.

DOI: 10.1103/PhysRevLett.118.050501

Superdense coding enables one qubit to carry two bits of information between a sender Alice and receiver Bob when they share an entanglement resource, perhaps distributed at “off-peak” times [1]. Alice can choose to use this quantum ability at a time of optimal advantage, after the time of distribution, when she and Bob have access to the quantum memory [2]. A significant challenge in realizing superdense coding is the need to perform a complete Bell-state measurement (BSM) on the photon pair, which is not possible using only linear optics and a single degree of shared entanglement [3,4]. While nonlinear optics [5] or the utilization of ancillary photons and linear optics [6] enable a complete BSM, these methods are challenged by inefficiency and impracticality. However, a complete BSM with linear optics can be performed by using entanglement in an ancillary degree of freedom (DOF), so-called hyperentanglement [7,8]. This ancillary DOF has no information encoded within it; rather, it enables a complete BSM by expanding the measurement space. Complete BSM implementations have been demonstrated previously using states hyperentangled in orbital angular momentum and polarization degrees of freedom [9] as well as with states hyperentangled in momentum and polarization [10]. However, these states are not compatible with transmission through fiber-based networks, which form the backbone of modern telecommunication systems. Previously, Schuck *et al.* have shown that time-polarization hyperentanglement can be used for a complete BSM [11], but required number-resolving detectors to identify the states completely. Yet this encoding is attractive in that it permits efficient transmission through an optical fiber and that some photon pair sources generate time entanglement for “free”.

In this Letter, we report results from an experimental demonstration of superdense coding over optical fiber links using a complete BSM based on time-polarization hyperentanglement. Our novel implementation requires only linear optics and common single-photon detectors. The resulting combination of a hyperentangled photon pair source and novel discrimination device yields an observed

channel capacity of 1.665 ± 0.018 , the highest reported to date for a single-qubit and linear optics. We demonstrate the feasibility of this setup by transmitting a 3.4 kB image that is recovered with 87% fidelity. This proof-of-principle milestone opens up the potential integration of practical superdense coding within the modern fiber-based telecommunication infrastructure [12].

We use the experimental configuration for the complete BSM shown in Fig. 1. The principle of operation behind the BSM device is to use the temporal and polarization coherences of the photon pair to produce unique detection outcomes for each of the four polarization-encoded Bell states:

$$|\Phi^\pm\rangle = (|H_0H_1\rangle \pm |V_0V_1\rangle)/\sqrt{2}, \quad (1)$$

$$|\Psi^\pm\rangle = (|H_0V_1\rangle \pm |V_0H_1\rangle)/\sqrt{2} \quad (2)$$

with H and V denoting horizontal and vertical polarization, respectively, and the subscripts 0 and 1 denoting the orthogonal spatial modes. The complete time-polarization hyperentangled states composed of two entangled polarization qubits and one time qudit of infinite dimension are

$$|\Phi^\pm(t)\rangle = |\Phi^\pm\rangle \otimes |\phi(t)\rangle, \quad (3)$$

$$|\Psi^\pm(t)\rangle = |\Psi^\pm\rangle \otimes |\phi(t)\rangle, \quad (4)$$

where t is the time since photon pair creation and $\int_{-\infty}^{\infty} \langle \phi(t) | \phi(t) \rangle dt = 1$. The entangled photons from one of the states given in Eq. (3) or (4) enter the interferometer in Fig. 1 and output to modes 2 and 3. As shown in Fig. 2, Hong-Ou-Mandel interference at this first beam splitter leads to a unique output for each of the four Bell-state inputs. Schuck *et al.* suggested a similar arrangement followed by photon number-resolving detection to identify the output state.

We avoid the need for photon number-resolving detectors by orchestrating the two-photon interference such that

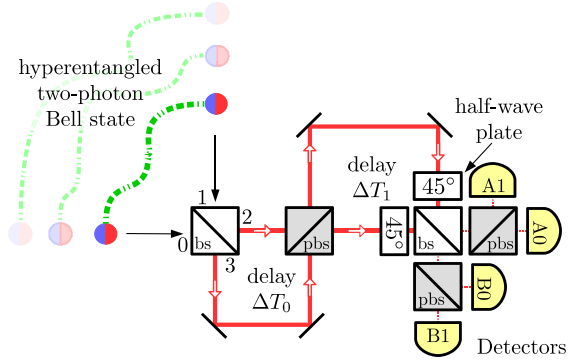


FIG. 1. Our complete Bell-state measurement is achieved using linear optics and time-polarization hyperentanglement. Two-photon interference is orchestrated to ensure Bell-state detection signatures do not involve two photons coincident on a single detector. bs \equiv beam splitter, and pbs \equiv polarizing beam splitter.

our unique BSM signatures do not involve the photon pair coincident at a detector—that would require a number-resolving detector to observe deterministically. The complete utilization of this interference requires the temporal modes $|\phi(t)\rangle$, $|\phi(t - \Delta T_0)\rangle$, $|\phi(t - \Delta T_1)\rangle$, and $|\phi(t - \Delta T_0 - \Delta T_1)\rangle$ to be indistinguishable, which is the case when the two-photon coherence time is much larger than the apparatus paths. When this interference is present, the four Bell states have three distinct photon pair relative detection times, delays. These delays are the result of Bob’s apparatus, not temporal modulations by Alice. As shown by Figs. 1 and 2, Φ^\pm states result in photon pair detections with no delay between photon time of arrival. This is necessary, since the photons in Φ^\pm states copropagate through the interferometer. By comparison, the Ψ^\pm state results in a relative time delay of ΔT_0 between members of the photon pair. This is due to the members taking separate paths in the first interferometer segment and their copropagation in the second segment. A similarly unique signature for the Ψ^- state arises when those photons copropagate in the first segment and take separate paths in the second segment of the apparatus. This requires the Ψ^- photon pair to have a relative time delay of ΔT_1 .

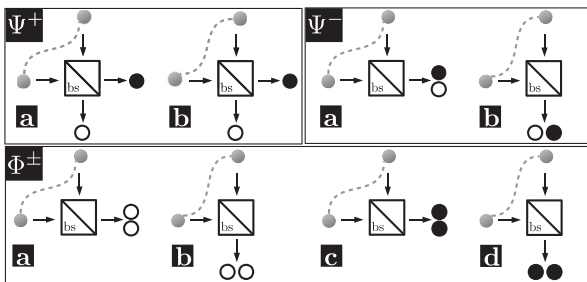


FIG. 2. Hong-Ou-Mandel interference at a beam splitter leads to unique outputs for the four Bell states. This leads to partial Bell-state discrimination, perfectly identifying Ψ^+ and Ψ^- from Φ states. The Φ^+ and Φ^- states are left indistinguishable.

The distinct propagation for each Bell state illustrates that our apparatus is a “four-in-one” two-photon interferometer that utilizes elements from several fundamental quantum information ideas including Hong-Ou-Mandel interference [13], partial Bell-state analysis [14], and time entanglement [15]. Unlike previous experiments that discard a portion of the quantum coherence by segregating outputs after the first beam splitter [11], we retain all coherence present to assist in the complete Bell-state discrimination. In conjunction with the aforementioned time signatures, the path-delayed two-photon interferometers ensure unique fully determinable detection outcomes that do not include two photons with the same polarization in the same output port, a limitation of a previous experiment [11].

We verify the design of the unique detection capabilities for this device by considering the symmetric beam splitter relations [11,16]

$$\begin{aligned} |H_0\rangle &\xrightarrow{BS} (|H_2\rangle + i|H_3\rangle)/\sqrt{2}, & |H_1\rangle &\xrightarrow{BS} (i|H_2\rangle + |H_3\rangle)/\sqrt{2}, \\ |V_0\rangle &\xrightarrow{BS} (|V_2\rangle - i|V_3\rangle)/\sqrt{2}, & |V_1\rangle &\xrightarrow{BS} (-i|V_2\rangle + |V_3\rangle)/\sqrt{2}, \end{aligned}$$

where the ports 0, 1, 2, and 3 are identified at the first beam splitter in Fig. 1. Additionally, the effect of a 45° polarization rotation on a single photon using a half-wave plate, a Hadamard gate, is modeled as

$$|H\rangle \xrightarrow{45^\circ} (|H\rangle + |V\rangle)/\sqrt{2}, \quad |V\rangle \xrightarrow{45^\circ} (|H\rangle - |V\rangle)/\sqrt{2}.$$

Given these relations, one may verify that, with phases $\omega\Delta T_0 = 2n\pi$ and $\omega\Delta T_1 = 2m\pi$, where n and m are integers, the output states for the four Bell states given by Eqs. (3) and (4) yield the interferometer output states

$$\begin{aligned} |\Phi^+\rangle &\rightarrow (|H_A V_A\rangle + |H_B V_B\rangle)/\sqrt{2}, \\ |\Phi^-\rangle &\rightarrow (|H_A H_B\rangle - |V_A V_B\rangle)/\sqrt{2}, \\ |\Psi^+\rangle &\rightarrow (|H_A H'_B\rangle + |H'_A H_B\rangle + |V_A V'_B\rangle + |V'_A V_B\rangle \\ &\quad + |H_A V'_B\rangle - |H'_A V_B\rangle + |V_A H'_B\rangle - |V'_A H_B\rangle)/\sqrt{8}, \\ |\Psi^-\rangle &\rightarrow (|H_A V''_A\rangle + |H''_A V_A\rangle - |H_B V''_B\rangle - |H''_B V_B\rangle \\ &\quad + i[|H_A V''_B\rangle - |H''_A V_B\rangle + |V_A H''_B\rangle - |V''_A H_B\rangle])/ \sqrt{8}, \end{aligned}$$

where A and B label the output ports and the prime and double prime indicate a ΔT_0 and ΔT_1 delayed photon, respectively. This set of outputs is smaller than what would be observed for photons separable in the temporal degree of freedom, i.e., photons that are not hyperentangled. A time-entangled photon pair can take one of multiple paths, 2–4 depending on the state, but these paths are indeterminable—they interfere upon leaving the interferometer. This interference and subsequent interferometer phase sensitivity allow us to choose the deterministic and measurable Bell-state

TABLE I. Bell-state detection signatures include a time Δt between photon detections, the same or different port detection, and the same (\parallel) or different (\perp) polarizations.

| | |
|----------|----------------------------------------------------------|
| Φ^+ | $\Delta t = 0$, \parallel ports, \perp polarization |
| Φ^- | $\Delta t = 0$, \perp ports, \parallel polarization |
| Ψ^+ | $\Delta t = \Delta T_0$, \perp ports |
| Ψ^- | $\Delta t = \Delta T_1$, \perp polarization |

detection signatures given in Table I. In addition to superdense coding, this novel BSM may serve as an entanglement witness for fiber-based quantum seal applications [17].

Our experimental implementation utilized an 810 nm entangled photon pair source characterized to produce each Bell state with 0.97 fidelity. The pair source is based on spontaneous parametric down-conversion using a potassium titanyl phosphate (PPKTP) nonlinear crystal within a Sagnac loop to produce a polarization-entangled biphoton state [18]. The temporal entanglement results from the long coherence time of the continuous-wave 405 nm diode laser pump. Pumping with 1.85 mW produced 2.27×10^5 pairs/s. Alice encodes each of the four Bell states utilizing two liquid

crystal wave plates. The first is oriented to apply an $I = \begin{pmatrix} 1 & 0 \\ 0 & 1 \end{pmatrix}$ or $X = \begin{pmatrix} 0 & 1 \\ 1 & 0 \end{pmatrix}$ gate, and the second applies an I or $Z = \begin{pmatrix} 1 & 0 \\ 0 & -1 \end{pmatrix}$ gate. Each combination II , IZ , XI , and XZ encodes one of the four Bell states. Because of losses, the coincident count rate observed by Bob was approximately 200 counts per second.

Given our timing resolution of 4 ns, we required the interferometer to have temporal delays $\Delta T_0 \approx 5$ ns and $\Delta T_1 \approx 10$ ns. Because of these large time delays, we chose to implement the experimental apparatus in a polarization-maintaining (PM) optical fiber as seen in Fig. 3. The fiber lengths needed for the first loop were 1 and 2 m, for the short and long paths, respectively, and, similarly, 2 and 4 m in the second loop. Each fiber path consists of two fibers of equal length orthogonally connected such that the macroscopic temporal effects of birefringence were compensated. Experimentally, we reconfigured a simple fiber connector such that the axes were aligned orthogonally. These connections are indicated in Fig. 3 as a \times symbol between two optical fibers. The use of the PM optical fiber requires that we take into account the microscopic difference in the phase due to birefringence in different paths. This phase compensation and the calibration of the phases needed to ensure unique BSM signatures is accomplished using liquid crystal wave plates. The phase of each photon polarization is individually modulated in the long path of the second loop, and the phase of one photon polarization is modulated in the short path of the second loop. Because of the long path lengths, the thermal drift of the fibers and frequency

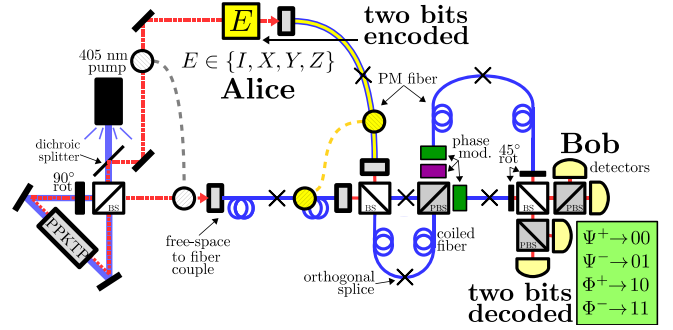


FIG. 3. To implement superdense coding, Alice and Bob initially each receive one photon from a time-polarization hyper-entangled photon pair. Alice performs one of four operations on her photon, which encodes two bits on the nonlocal two-photon Bell state. Alice transmits her photon to Bob, who performs a Bell-state measurement, i.e., decodes two bits. bs \equiv beam splitter, pbs \equiv polarizing beam splitter, and PPKTP \equiv potassium titanyl phosphate.

drift of the pump laser limit stable operation to approximately 100 s before recalibration is necessary. We characterized the BSM performance by calibrating the interferometer to the optimal discrimination settings, preparing each of the four Bell states, and recording the state detected by the apparatus. In estimating the success probabilities, we recorded approximately 800 detection signatures for each state, which occurred over a 5 s interval. The raw data collected are given in Table II. The maximum-likelihood estimates for the conditional probabilities with accidental coincidences included are given in Fig. 4.

The channel capacity C [19] is the maximum mutual information $I(x; y)$ possible for a given set of conditional probabilities $p(y|x)$, where x is the state prepared by Alice and y is the state decoded by Bob. This capacity is

$$C = \max_{p(x)} \sum_{y=0}^3 \sum_{x=0}^3 p(y|x) p(x) \log \left(\frac{p(y|x)}{\sum_{x'=0}^3 p(y|x') p(x')} \right),$$

TABLE II. The 5 s counts of received state y given sent state x .

| x | y | | | |
|----------|----------|----------|----------|----------|
| | Φ^- | Φ^+ | Ψ^- | Φ^+ |
| Φ^- | 710 | 8 | 8 | 4 |
| Φ^+ | 7 | 715 | 9 | 13 |

| x | y | | | |
|----------|----------|----------|----------|----------|
| | Φ^- | Φ^+ | Ψ^- | Φ^+ |
| Ψ^- | 15 | 8 | 748 | 9 |
| Ψ^+ | 34 | 23 | 15 | 840 |

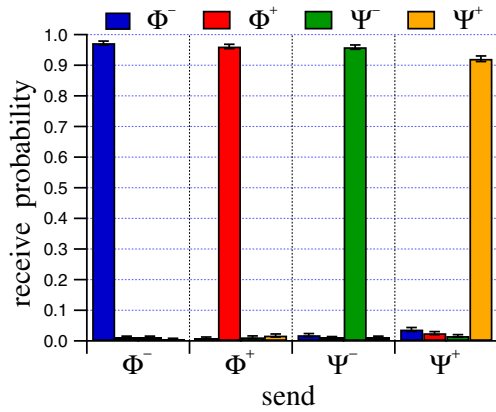


FIG. 4. The conditional probabilities $p(y|x)$ of receiving state y given the sent state x using our apparatus give the highest channel capacity to date, 1.665 ± 0.018 , by encoding on a single qubit and decoding using linear optics.

where $p(\mathbf{x}) = \{p(\Phi^-), p(\Phi^+), p(\Psi^-), p(\Psi^+)\}$ maximizes the capacity. For the conditional probabilities given in Fig. 4, we find the channel capacity to be 1.665 ± 0.018 for arguments $p(\Phi^-) = 0.262$, $p(\Phi^+) = 0.256$, $p(\Psi^-) = 0.256$, and $p(\Psi^+) = 0.226$. The maximum channel capacity possible using linear optics, a single qubit, and a single degree of entanglement is 1.585 [20]. Our experiment has exceeded this bound as well as the previous highest channel capacity reported for encoding on a single qubit and decoding using linear optics [9].

We next demonstrate the use of superdense coding as part of a hybrid, quantum-classical protocol for communicating between users Alice and Bob. We make use of conventional optical network communication between two users to coordinate Alice’s quantum transmitter and Bob’s quantum receiver [22,23]. The basic steps in the protocol for this demonstration are (1) Alice transmits a classical send request to Bob; (2) Bob returns a classical acknowledgement to Alice; (3) Alice transmits two bits using superdense coding; (4) Bob receives and decodes the two-bit message; and (5) Bob transmits a classical receipt to Alice. This protocol is repeated n times, until Alice has completed the transmission of a $2n$ -bit message to Bob. Because of the spontaneous nature of the photon pair source, only the first photon pair detected during step 3 above is used, even though other photon pairs may be detected. In this regard, the classical messages before and after a burst of superdense coding act to frame each two-bit message. While this incurs a large overhead, it ensures the detected bits are properly framed, so that the transmitted message can be reliably constructed. A less conservative protocol would permit Alice to transmit multiple two-bit messages uninterrupted and require Bob to properly partition this sequence into the corresponding frames.

As a demonstration of the system capabilities, we have transmitted the 3.4 kB image shown in Fig. 5 (left). The corresponding received image is shown in Fig. 5 (right).

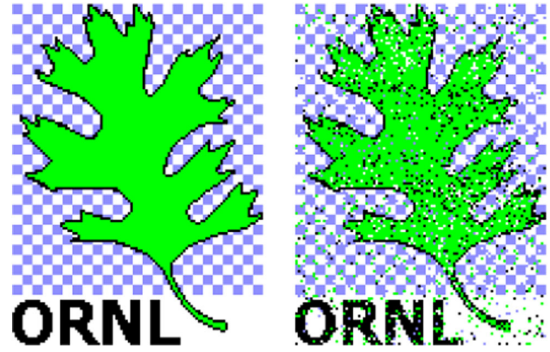


FIG. 5. (Left) The original four-color 100×136 pixel 3.4 kB image. (Right) The image received using superdense coding. The calculated fidelity was 87%.

The received image is calculated to have a fidelity of 87%. The errors in the received image result from drift in the interferometer during transmission, phase miscalibration, and imperfect state generation. It should be apparent that the fidelity of the received image is less than that of the optimal characterization presented in Fig. 4. This is due to performance trade-offs in the system operation that reduce the collection time at the expense of reduced detection fidelity. For the current demonstration, the effective bit rate during operation that included a classical send message, phase encoding using liquid crystal wave plates, a classical receive message, and periodic calibration was 1 bit/s. The fiber link for this system was 2 m of PM optical fiber. We do not foresee any fundamental impediments to using longer optical fibers beyond increased losses and cost. In particular, an implementation using a standard single-mode fiber could operate by using a polarization correction or stabilization system.

Our experiment could be improved by reducing the spontaneity of the source by utilizing a pulsed pump laser, in which case the temporal delays in the interferometer would need to be multiples of the pulse period t_p , for instance, $\Delta T_0 = t_p$ and $\Delta T_1 = 2t_p$. Achieving a finer time resolution would allow for smaller delays ΔT_0 and ΔT_1 which would improve the stability; i.e., the drift would be reduced. Packaging the device or using integrated optics would substantially increase the bit rate by reducing the photon pair loss due to free space to fiber-coupling inefficiencies. The speed of Alice’s encoding is limited by the response time of the liquid crystal wave plates, which is on the order of milliseconds. Faster options include lithium-niobate phase modulators [24], which can achieve modulation speeds on the order of nanoseconds.

In conclusion, we have achieved a single-qubit channel capacity of 1.665 ± 0.018 over optical fiber links enabled by a complete BSM using linear optics, hyperentanglement, and common single-photon detectors. This channel capacity is the highest to date for encoding on a single qubit and decoding using linear optics. Our novel interferometric design allows “off-the-shelf” single-photon detectors to

enable the complete Bell-state discrimination instead of the number-resolving detectors required by previous experiments [11]. To our knowledge, this is the first demonstration of superdense coding over an optical fiber and a step towards the practical realization of superdense coding. Alongside our demonstration of a hybrid quantum-classical transfer protocol, these results represent a step toward the future integration of quantum communication with fiber-based networks [25,26].

This work was supported by the United States Army Research Laboratory. This Letter has been authored by UT-Battelle, LLC under Contract No. DE-AC05-00OR22725 with the U.S. Department of Energy. The United States Government retains and the publisher, by accepting the article for publication, acknowledges that the United States Government retains a nonexclusive, paid-up, irrevocable, worldwide license to publish or reproduce the published form of this manuscript, or allow others to do so, for United States Government purposes. The Department of Energy will provide public access to these results of federally sponsored research in accordance with the DOE Public Access Plan.

*williamsbp@ornl.gov

†sadierrj@ornl.gov

‡humblerts@ornl.gov

- [1] C. H. Bennett and S. J. Wiesner, *Phys. Rev. Lett.* **69**, 2881 (1992).
- [2] A. I. Lvovsky, B. C. Sanders, and W. Tittel, *Nat. Photonics* **3**, 706 (2009).
- [3] N. Lütkenhaus, J. Calsamiglia, and K.-A. Suominen, *Phys. Rev. A* **59**, 3295 (1999).
- [4] L. Vaidman and N. Yoran, *Phys. Rev. A* **59**, 116 (1999).
- [5] Y.-H. Kim, S. P. Kulik, and Y. Shih, *Phys. Rev. Lett.* **86**, 1370 (2001).
- [6] W. P. Grice, *Phys. Rev. A* **84**, 042331 (2011).
- [7] P. G. Kwiat, *J. Mod. Opt.* **44**, 2173 (1997).
- [8] J. T. Barreiro, N. K. Langford, N. A. Peters, and P. G. Kwiat, *Phys. Rev. Lett.* **95**, 260501 (2005).
- [9] J. T. Barreiro, T.-C. Wei, and P. G. Kwiat, *Nat. Phys.* **4**, 282 (2008).
- [10] M. Barbieri, G. Vallone, P. Mataloni, and F. De Martini, *Phys. Rev. A* **75**, 042317 (2007).
- [11] C. Schuck, G. Huber, C. Kurtsiefer, and H. Weinfurter, *Phys. Rev. Lett.* **96**, 190501 (2006).
- [12] V. R. Dasari, R. J. Sadlier, R. Prout, B. P. Williams, and T. S. Humble, *Proc. SPIE Int. Soc. Opt. Eng.* **9873**, 98730B (2016).
- [13] C. K. Hong, Z. Y. Ou, and L. Mandel, *Phys. Rev. Lett.* **59**, 2044 (1987).
- [14] H. Weinfurter, *Europhys. Lett.* **25**, 559 (1994).
- [15] J. D. Franson, *Phys. Rev. Lett.* **62**, 2205 (1989).
- [16] Z.-Y. J. Ou, *Multi-photon Quantum Interference* (Springer, New York, 2007).
- [17] B. P. Williams, K. A. Britt, and T. S. Humble, *Phys. Rev. Applied* **5**, 014001 (2016).
- [18] T. Kim, M. Fiorentino, and F. N. C. Wong, *Phys. Rev. A* **73**, 012316 (2006).
- [19] T. M. Cover and J. A. Thomas, *Elements of Information Theory* (Wiley, New York, 2012).
- [20] We note that methods have been proposed to achieve a channel capacity of 2 utilizing linear optics and one photon on average [21].
- [21] P. Lougovski and D. B. Uskov, *Phys. Rev. A* **92**, 022303 (2015).
- [22] T. S. Humble and R. J. Sadlier, *Opt. Eng. (Bellingham, Wash.)* **53**, 086103 (2014).
- [23] R. J. Sadlier and T. S. Humble, *Quantum Meas. Quantum Metrology* **3**, 1 (2016).
- [24] E. L. Wooten, K. M. Kissa, A. Yi-Yan, E. J. Murphy, D. A. Lafaw, P. F. Hallemeier, D. Maack, D. V. Attanasio, D. J. Fritz, G. J. McBrien, and D. E. Bossi, *IEEE J. Sel. Top. Quantum Electron.* **6**, 69 (2000).
- [25] T. S. Humble, *IEEE Commun. Mag.* **51**, 56 (2013).
- [26] V. R. Dasari and T. S. Humble, [arXiv:1512.08545](https://arxiv.org/abs/1512.08545).